Synthesis of Nickel Nanoparticles in Water-in-Oil Microemulsions

Dong-Hwang Chen* and Szu-Han Wu

Department of Chemical Engineering, National Cheng Kung University, Tainan, Taiwan 701, R.O.C.

Received October 29, 1999

The synthesis of nickel nanoparticles by the reduction of nickel chloride with hydrazine in the cationic water-in-oil microemulsions of water/CTAB (cetyltrimethylammonium bromide)/*n*-hexanol at 73 °C has been studied. By the analyses of electron diffraction pattern and X-ray diffraction, the resultant particles were characterized to be the pure nickel crystalline with a face-centered cubic (fcc) structure. The investigation on the composition of microemulsion solution indicated that the average diameter of nickel nanoparticles was affected mainly by the ratio of CTAB to *n*-hexanol instead of the size of microemulsion droplets. Smaller particles could be obtained at higher ratios of CTAB to *n*-hexanol. At a constant nickel chloride concentration, the average diameter of nickel nanoparticles decreased with the increase of hydrazine concentration and then approached to a constant value when the concentration ratio of hydrazine to nickel chloride was above 10. At a sufficient high hydrazine concentration, the average diameter of nickel nanoparticles was independent of nickel chloride concentration. The effects of microemulsion composition and the concentrations of hydrazine and nickel chloride on the particle size are discussed in detail. The magnetic measurements for a typical sample with an average diameter of 4.6 nm showed that the resultant nickel nanoparticles were superparamagnetic due to extremely small size. The saturation magnetization (26.2 emu/g), remanent magnetization (0.67 emu/g), and the coercivity (7.5 Oe) were significantly smaller than those of the bulk nickel, reflecting the nanoparticle nature. In addition, the magnetization was observed to increase with the decrease of temperature due to the decrease in thermal energy.

Introduction

In recent years, the preparation, characterization, and applications of the nanosized materials have received increasing attention from many researchers in various fields, e.g., chemistry, physics, material science, biology, and the corresponding engineerings.[1−3] Since the nanoparticles usually exhibit unusual electronic, optical, magnetic, and chemical properties significantly different from those of the bulk materials due to their extremely small sizes and large specific surface areas, they have various potential applications such as catalysis, electronic, optical, and mechanic devices, magnetic recording media, superconductors, high-performance engineering materials, dyes, pigments, adhesives, photographic suspensions, drug delivery, and so on.[3−7]

A number of techniques have been used for the production of nanoparticles, such as gas-evaporation,[8] sputtering,[9] coprecipitation,[10] sol−gel method,[11] hydrothermal,[12] microemulsion,[3,13−15] and so on. Water-in-oil (w/o) microemulsion solutions are transparent, isotropic liquid media with nanosized water droplets that are dispersed in a continuous oil phase and stabilized by surfactant molecules at the water/oil interface. These surfactant-covered water pools offer a unique microen-

* Telephone: 886-6-2757575 ext. 62680. Fax: 886-6-2344496. E-mail: chendh@mail.ncku.edu.tw.

(1) (a) Ozin, G. A. *Adv. Mater.* **1992**, *4*, 612. (b) Ozin, G. A. *Science* **1996**, *271*, 920−941. (c) Cahn, R. W. *Nature* **1992**, *359*, 591.

(2) (a) Hayashi, C. *Phys. Today* **1987**, *40*, 44. (b) Gleiter, H. *Prog. Mater. Sci.* **1989**, *33*, 223. (c) Uyeda, R. *Prog. Mater. Sci.* **1991**, *35*, 1.

(3) (a) Fendler, J. H. *Chem. Rev.* **1987**, *87*, 877. (b) Henglein, A. *Chem. Rev.* **1989**, *89*, 1861.

(4) (a) Dagani, R. *Chem. Eng. News* **1992**, Nov 23, 18. (b) Dagani, R. *Chem. Eng. News* **1999**, (June 7), 25. (c) Colvin, V. L.; Schlamp, M. C.; Alivisatos, A. P. *Nature* **1994**, *370*, 354. (d) Hamilton, J. F.; Baetzold, R. C. *Science* **1979**, *205*, 1213.

(5) (a) Schmid, G. *Chem. Rev.* **1992**, *92*, 1709. (b) Kamat, P. V. *Chem. Rev.* **1993**, *93*, 267. (c) Lewis, L. N. *Chem. Rev.* **1993**, *93*, 2693. (d) Gates, B. C. *Chem. Rev.* **1995**, *95*, 511.

(6) (a) Andres, R. P.; Averback, R. S.; Brown, W. L.; Brus, L. E.; Goddard, W. A., III; Kaldor, A.; Louie, S. G.; Moscovits, M.; Peercy, P. S.; Riley, S. J.; Siegel, R. W.; Spaepen, F.; Wang, Y. *J. Mater. Res.* **1989**, *4*, 704. (b) Han, Y. T. *MRS Bull.* **1989**, *14*, 13. (c) Siegel, R. W. *MRS Bull.* **1990**, *15*, 60. (d) Beecroft, L. L.; Ober, C. K. *Chem. Mater.* **1997**, *9*, 1302. (e) Yonezawa, T.; Toshima, N. *J. Chem. Soc., Faraday Trans.* **1995**, *91*, 4111.

(7) (a) Brus, L. *J. Phys. Chem.* **1986**, *90*, 2555. (b) Hoffman, A. J.; Mills, G.; Yee, H.; Hoffmann, M. R. *J. Phys. Chem.* **1992**, *96*, 5546. (c) Hailstone, R. K. *J. Phys. Chem.* **1995**, 99, 4414. (d) Lee, A. F.; Baddeley, C. J.; Hardacre, C.; Ormerod, R. M.; Lambert, R. M.; Schmid, G.; West, H. *J. Phys. Chem.* **1995**, *99*, 6096.

(8) (a) Siegel, R. W. *J. Mater. Res.* **1998**, *3*, 1367. (b) Uyeda, R. *J. Cryst. Growth* **1974**, *24*, 69.

(9) Fayet, P.; Woste, L. *Z. Phys. D* **1986**, *3*, 177.

(10) Tang, Z. X.; Sorensen, C. M.; Klabunde, K. J.; Hadjipanayis, G. C. *J. Colloid Interface Sci.* **1991**, *146*, 38.

(11) Fegley, B., Jr.; White, P.; Bowen, H. K. *Am. Ceram. Soc. Bull.* **1985**, *64*, 1115.

(12) Komarneni, S.; Roy, R.; Breval, E.; Ollinen, M.; Suwa, Y. *Adv. Ceram. Mater.* **1986**, *1*, 87.

(13) Osseo-Asare, K.; Arriagada, F. J. *Ceram. Trans.* **1990**, *12*, 3.

(14) Pileni, M. P. *J. Phys. Chem.* **1993,** *97*, 6961.

(15) Pillai, V.; Kumar, P.; Hou, M. J.; Ayyub, P.; Shah, D. O. *Adv. Colloid Interface Sci.* **1995**, *55*, 241.

10.1021/cm991167y CCC: $19.00
Published on Web 04/05/2000

vironment for the formation of nanoparticles. They not only act as microreactors for processing reactions but also inhibit the excess aggregation of particles because the surfactants could adsorb on the particle surface when the particle size approaches to that of water pool. As a result, the particles obtained in such a medium are generally very fine and monodispersed.[16−18]

Since the platinum-group metal nanoparticles were successfully synthesized in w/o microemulsions by Boutonnet et al.,[19] the microemulsion technique has been widely used to prepare nanoparticles of numerous materials, including metals,[19−24] metal sulfides and selenides,[25−29] metal borides,[30,31] metal carbonates,[32] metal halides,[33] metal oxides and hydroxides,[34−39] and organic polymers.[40] However, the preparations of some metal nanoparticles such as nickel, cobalt, and iron are more difficult. Nickel nanoparticles have attracted much attention because of their applications as catalysts and conducting or magnetic materials, but their preparation in w/o microemulsions has not been reported.

This article describes the synthesis of nickel nanoparticles in the cationic w/o microemulsion of water/CTAB (cetyltrimethylammonium bromide)/*n*-hexanol by the reduction of nickel chloride with hydrazine at an elevated temperature. The particle size and structure of the resultant nanoparticles have been characterized by transmission electron microscopy (TEM), electron diffraction pattern, and X-ray diffraction (XRD). The effects of microemulsion composition and the concentrations of nickel chloride and hydrazine on particle sizes have been investigated and discussed. The magnetic properties of the nickel nanoparticles have also been examined by the superconducting quantum interference device (SQUID) magnetometer.

Experimental Section

The cationic surfactant CTAB was obtained from Acros Organics (Belgium). Hydrazinium hydroxide and ammonia solution (28%) were the guaranteed reagents of E. Merck (Darmstadt). Nickel chloride was the product of Hayashi (Osaka). *n*-Hexanol was supplied by TEDIA (Fairfield). The water used throughout this work was the reagent-grade water produced by Milli-Q SP ultrapure water purification system of Nihon Millipore Ltd., Tokyo.

Two types of microemulsion solutions were prepared by solubilizing aqueous $NiCl_2$ or N_2H_4 solution into a CTAB/*n*-hexanol mixture. The microemulsion compositions were selected according to the phase diagram of the ternary system water/CTAB/*n*-hexanol which could be found elsewhere.[30] The pH value of aqueous N_2H_4 solution was adjusted to be 13 with ammonia solution. The concentrations of $NiCl_2$ and N_2H_4 given in the text were based on the volume of aqueous solution instead of the total volume. The preparation of nickel nanoparticles was achieved by mixing rapidly the same volumes of two w/o microemulsion solutions, with $NiCl_2$ solubilized in one solution and N_2H_4 as the reducing agent in the other solution. The reduction reaction could be expressed as

$$2Ni^{2+} + N_2H_4 + 4OH^- \rightarrow 2Ni + N_2 + 4H_2O \qquad (1)$$

The preliminary experiments indicated that no significant reaction occurred at 25 °C even after several days, while the overall reaction including the reduction of nickel ions and the nucleation and growth of nickel nanoparticles was completed after 2 h at 40 °C and within 1 h above 70 °C. The selection of an appropriate reaction temperature and the addition of ammonia solution were two key points that the nickel nanoparticles could be prepared in the microemulsion system. In addition, it was observed that the resultant nickel nanoparticles could be well-dispersed in the microemulsion system over 1 month. Accordingly, all of the experiments were carried out at 73 °C, and the samples for the particle size, structural, and magnetic analyses were withdrawn after 1 h throughout this work.

It is notable that the preliminary experiments showed that no matter whether the synthesis reaction was performed in an inert atmosphere (N_2 gas) or not, only metallic nickel nanoparticles were obtained. No oxides or hydroxide such as NiO, Ni_2O_3, and $Ni(OH)_2$ were observed from the phase analysis by XRD. Since it was observed that N_2 gas was produced and bubbled up continuously during reaction as revealed by eq 1, it could be suggested that the N_2 gas produced might autocreate an inert atmosphere, and hence the input of extra N_2 gas was not necessary. So, no extra N_2 gas was input for the synthesis of nickel nanoparticles in this study.

The particle sizes were determined by TEM using a Hitachi model HF-2000 field emission transmission electron microscope with a resolution of 0.1 nm. The sample for TEM analysis was obtained by placing a drop of the dispersed solution onto a Formvar-covered copper grid and evaporated in air at room temperature. Before withdrawing the samples, the dispersed solutions were sonicated for 1 min to obtain better particle dispersion on the copper grid. For each sample, usually over 100 particles from different parts of the grid were used to estimate the average diameter and size distribution of particles. XRD measurements were performed on a Rigaku D/max III.V X-ray diffractometer using Cu−Kα radiation ($\lambda = 0.1542$ nm). The sample for XRD analysis was prepared by first adding the mixed solution of methanol and chloroform (1:1) to the microemulsion solution to cause phase separation, then

(16) Luisi, P. L.; Magid, L. J. *CRC Crit. Rev. Biochem.* **1986**, *20*, 409.
(17) Pileni, M. P., Ed. *Structure and Reactivity in Reverse Micelles*; Elsevier: Amsterdam, 1989.
(18) Paul, B. K.; Moulik, S. P. *J. Dispersion Sci. Technol.* **1997**, *18*, 301.
(19) Boutonnet, M.; Kizling, J.; Stenius, P.; Maire, G. *Colloids Surf.* **1982**, *5*, 209.
(20) Kurihara, K.; Kizling, J.; Stenius, P.; Fendler, J. H. *J. Am. Chem. Soc.* **1983**, *105*, 2574.
(21) Petit, C.; Lixon, P.; Pileni, M.-P. *J. Phys. Chem.* **1993**, *97*, 12974.
(22) Robinson, B. H.; Khan-Iodhi, A. N.; Towey, T. In *Structure and Reactivity in Reverse Micelles*; Pileni, M. P., Ed.; Elsevier: Amsterdam, 1989.
(23) Qi, L.; Ma, J.; Shen, J. *J. Colloid Interface Sci.* **1997**, *186*, 498.
(24) (a) Chen, D. H.; Wang, C. C.; Huang, T. C. *J. Colloid Interface Sci.* **1999**, *210*, 123. (b) Chen, D. H.; Yeh, J. J.; Huang, T. C. *J. Colloid Interface Sci.* **1999**, *215*, 159.
(25) Lianos, P.; Thomas, J. K. *J. Colloid Interface Sci.* **1987**, *117*, 505.
(26) Kortan, A. R.; Hull, R.; Opila, R. L.; Bawendi, M. G.; Steigerwald, M. L.; Carroll, P. J.; Brus, L. E. *J. Am. Chem. Soc.* **1990**, *112*, 1327.
(27) Ward, A. J. I.; O'Sullivan, E. C.; Rang, J.-C.; Nedeljkovic, J.; Patel, R. C. *J. Colloid Interface Sci.* **1993**, *161*, 316.
(28) Hirai, T.; Shiojiri, S.; Komasawa, I. *J. Chem. Eng. Jpn.* **1994**, *27*, 590.
(29) Haram, S. K.; Mahadeshwar, A. R.; Dixit, S. G. *J. Phys. Chem.* **1996,** *100*, 5868.
(30) Nagy, J. *Colloids Surf.* **1989**, *35*, 201.
(31) Lufimpadio, N.; Nagy, J. B.; Derouane, E. G. In *Surfactants in Solution*, Vol. 3; Mittal, K. L., Lindman, B. L., Eds.; Plenum: New York, 1984; pp 1483−1497.
(32) Kandori, K.; Kon-No, K.; Kitahara, A. *J. Colloid Interface Sci.* **1988**, *122*, 78.
(33) Dvolaitzky, M.; Ober, R.; Taupin, C.; Anthore, R.; Auvray, X.; Petipas, C.; Williams, C. *J. Dispersion Sci. Technol.* **1983**, *4*, 29.
(34) Osseo-Asare, K.; Arriagada, F. J. *Colloids Surf.* **1990**, *50*, 321.
(35) Ayyub, P.; Maitra, A. N.; Shah, D. O. *Phys. C.* **1990**, *168*, 571.
(36) Pillai, V.; Kumar, P.; Multani, M. S.; Shah, D. O. *Colloids Surf. A.* **1993**, *80*, 69.
(37) Joselevich, E.; Willner, I. *J. Phys. Chem.* **1994**, *98*, 7628.
(38) Chhabra, V.; Lal, M.; Maitra, A. N.; Ayyub, P. *Colloid Polym. Sci.* **1995**, *273*, 939.
(39) Chang, C.-L.; Fogler, H. S. *AIChE J.* 1996, **42**, 3153; *Langmuir* **1997**, *13*, 3295.
(40) Antonietti, M.; Basten, R.; Lohmann, S. *Macromol. Chem. Phys.* **1995,** *196*, 441.

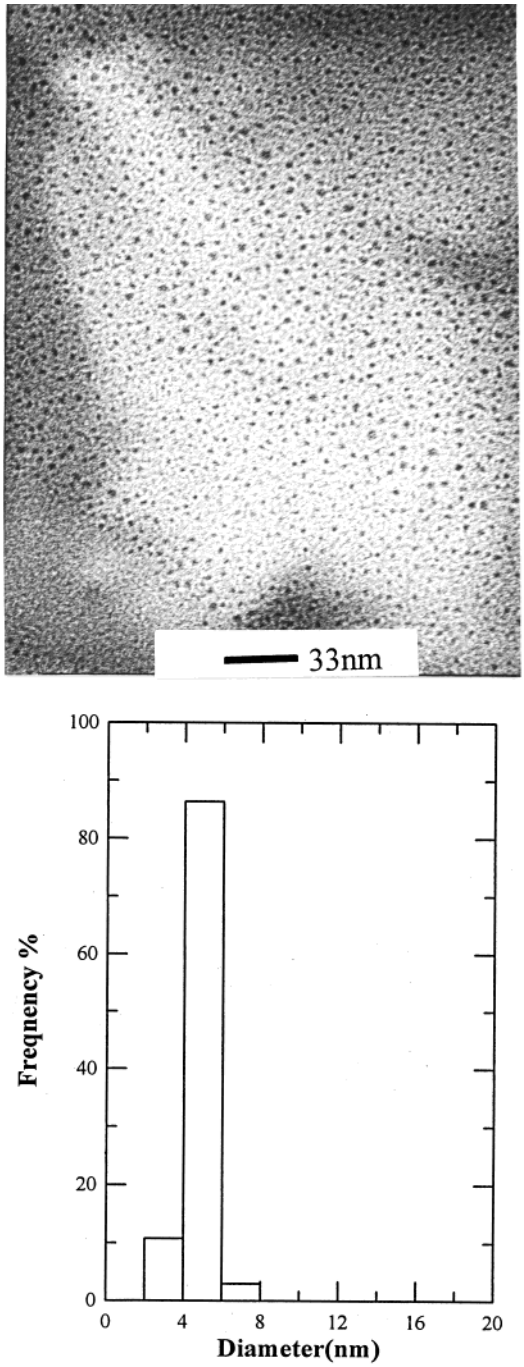

Figure 1. Transmission electron micrograph and size distribution of nickel nanoparticles. $[NiCl_2] = 0.05$ M; $[N_2H_5OH] = 1.0$ M; water/CTAB/*n*-hexanol = 22/33/45; 73 °C.

centrifuging the mixture, and finally drying the obtained precipitates. The magnetic measurements were done using a SQUID magnetometer (MPMS7, Quantum Design), and the samples were prepared using the same method as that for XRD analysis.

Results and Discussion

Structural Characterization. A typical transmission electron micrograph and the size distributions for the nickel nanoparticles obtained at a microemulsion system of water/CTAB/*n*-hexanol = 22/33/45 were shown in Figure 1. The particles essentially were monodispersed with an average diameter of 4.2 nm and a standard deviation of 0.7 nm. The corresponding electron diffraction pattern was indicated in Figure 2. Three fringe patterns with plane distances of 2.03, 1.76, and 1.02 Å could be observed. They are consistent with the indices (111), (200), and (222) of pure face-centered cubic (fcc) nickel. In addition, the XRD spectrum for the resultant particles was shown in Figure 3. Three characteristic peaks for nickel (2θ = 44.5, 51.8, and 76.4), marked by their indices ((111), (200), and (222)), were observed. This also revealed that the resultant particles were pure fcc nickel. In accordance with the above three analyses, it could be concluded that the nanoparticles prepared in this work were pure nickel of fcc structure.

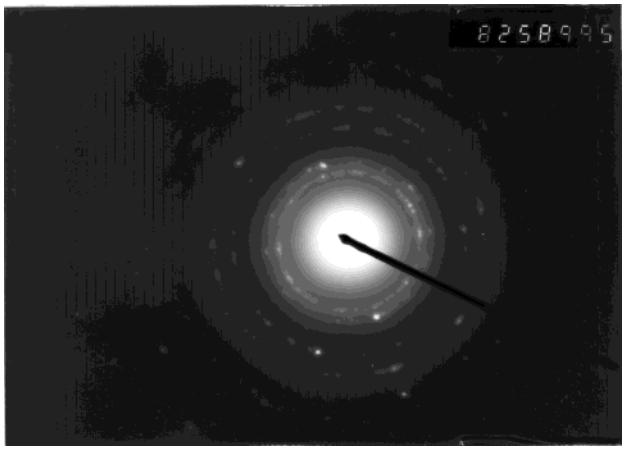

Figure 2. Electron diffraction pattern of nickel nanoparticles. $[NiCl_2] = 0.05$ M; $[N_2H_5OH] = 1.0$ M; water/CTAB/*n*-hexanol = 22/33/45; 73 °C.

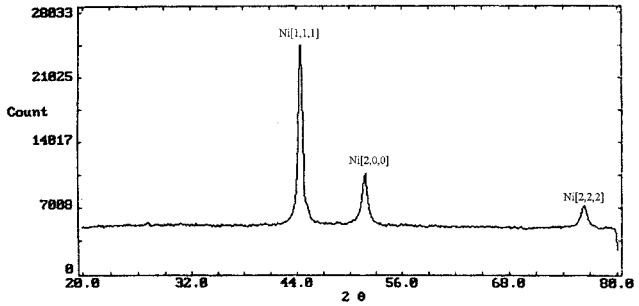

Figure 3. X-ray diffraction spectrum of nickel nanoparticles. $[NiCl_2] = 0.05$ M; $[N_2H_5OH] = 1.0$ M; water/CTAB/*n*-hexanol = 22/33/45; 73 °C.

Although it is known that nickel is easily oxidized to be oxides or hydroxide by water, some possible oxides or hydroxide such as NiO, Ni_2O_3, and $Ni(OH)_2$ were not observed in this study. This might be due to the fact that the reaction autocreated an inert atmosphere and was carried out at appropriate pH, temperature, and hydrazine concentration. However, the water confined in the microemulsion droplets usually has significantly lower activity than the bulk water because the average diameters of microemulsion droplets are very small (only several nanometers). This might be another possible reason that no oxides or hydroxide were formed.

Effects of Preparation Conditions. As has been known, the size of microemulsion droplets was dependent on the solution composition. When the particle diameter reached that of the microemulsion droplet, the surfactant molecules might adsorb on the surface of the particle formed therein. They act as a protective agent

Table 1. Effect of Microemulsion Composition on Average Diameters of Nickel Nanoparticles

microemul. comp. (wt %) water/CTAB/ *n*-hexanol	CTAB/water (wt %/wt %)	CTAB/*n*-hexanol (wt %/wt %)	av diam. nickel nanopart. (nm)
18/27/55		0.49	14.3 ± 1.5
20/30/50	1.5	0.60	4.6 ± 0.8
22/33/45		0.73	4.2 ± 0.7
10/20/70		0.29	8.2 ± 0.7
16/32/52	2	0.61	8.2 ± 0.5
18/36/46		0.78	5.8 ± 0.5

and restricted the growth of nanoparticles. Therefore, the composition of microemulsion solution affects not only the stability of microemulsion system but also the formation of nanoparticles. According to the phase diagram of the ternary system water/CTAB/*n*-hexanol,[30] several microemulsion compositions as shown in Table 1 were selected for the preparation of nickel nanoparticles in this study.

The average diameters for all of the nickel nanoparticles obtained at various microemulsion compositions were indicated in Table 1. It was obvious that the average diameters of nickel nanoparticles decreased with the increase of water content at the weight ratios CTAB/water = 1.5 and 2. Nagy[30] studied the relationships between the solution composition and the microemulsion droplets for the ternary system water/CTAB/*n*-hexanol by using NMR. As expected, he found that the diameter of the microemulsion droplet increased with the increase of water content due to the increase of the total volume of water and to the concomitant decrease of the total surface of the aggregate. Thus, the phenomenon observed in this study, which indicated the average diameters of nickel nanoparticles decreased with the increase of the diameters of microemulsion droplets, was a little unexpected and seemed not consistent with the basic function of microemulsion droplets to provide a limited volume for the formation of nanoparticles. However, in fact, Lufimpadio et al.[31] also observed the similar phenomenon in the preparation of iron boride nanoparticles in the water/CTAB/*n*-hexanol system. Therefore, in addition to the size of microemulsion droplets, there must be other factors affecting strongly the size of nickel nanoparticles formed in the water/CTAB/*n*-hexanol microemulsion.

In this study, the typical water content in the microemulsion was about 20%, and the maximum concentration of nickel chloride used was 0.05 M based on the volume of aqueous solution. According to eq 1, the water produced was only about 0.18% of the original water content. So, the changes in water content or the number density of microemulsion droplets should be negligible.

From another viewpoint, as shown in Table 1, the decrease of water content means the increase of *n*-hexanol content or the decrease of the weight ratio of CTAB to *n*-hexanol at a constant weight ratio of CTAB to water. Since the interface was composed of CTAB and *n*-hexanol molecules, the decreased weight ratio of CTAB to *n*-hexanol would lead to the dilution of interface, reduce the interaction between CTAB molecules, and result in a more labile interface. The greater mobility of the interface favored the rearrangement of the microemulsion droplets and led to the formation of larger particles. In addition, the microemulsion droplets

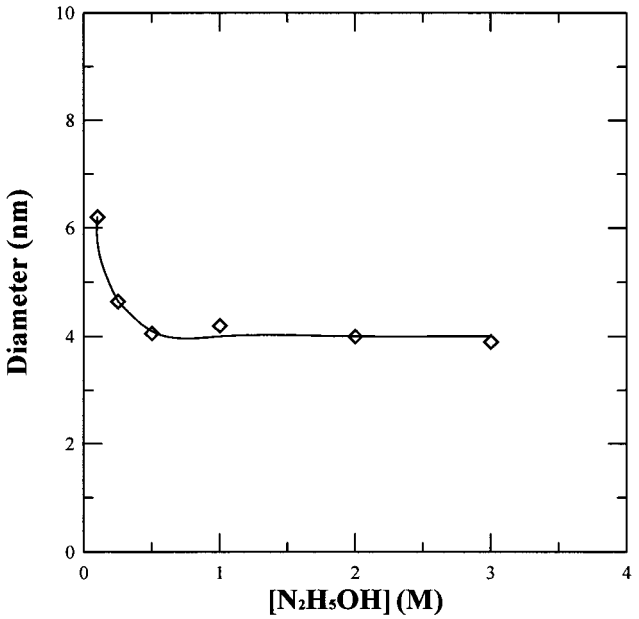

Figure 4. Effect of hydrazine concentration on the size of nickel nanoparticles. [$NiCl_2$] = 0.05 M; water/CTAB/*n*-hexanol = 22/33/45; 73 °C.

were dynamic and the size of the particles formed therein might be larger than that of microemulsion droplets. Therefore, although the microemulsion droplets provided a limited microenvironment, the key factor for the preparation of smaller nickel nanoparticles in the water/CTAB/*n*-hexanol system seemed be the higher weight ratio of CTAB to *n*-hexanol instead of the smaller microemulsion droplets.

The effect of hydrazine concentration on the size of the resultant nickel nanoparticles was investigated in the microemulsion system of water/CTAB/*n*-hexanol = 22/33/45. The concentration of nickel chloride in the aqueous phase was fixed at 0.05 M. Figure 4 showed that the average diameters of nickel nanoparticles decreased with the increase of hydrazine concentration and approached to a constant value when the hydrazine concentration was above 0.5 M, i.e., [N_2H_5OH]/[$NiCl_2$] > 10. This phenomenon could be explained from the influence of reduction rate on the nucleation.

Since a minimum number of atoms was required to form a stable nucleus, a collision between several atoms must occur for a nucleation. However, the probability was much lower than the probability for the collision between one atom and a nucleus already formed. That is, once the nuclei were formed, the growth process would be superior to the nucleation. In addition, the resultant nanoparticles were essentially monodispersed. So, it might be suggested that all of the nuclei were formed almost at the same time and grew at the same rate. Thus, the number of the nuclei formed at the very beginning of the reduction determined the number and size of the resultant particles. At a low hydrazine concentration, the reduction rate of nickel chloride was slow and only few nuclei were formed at the early period of the reduction. The atoms formed at the latter period were used mainly to the collision with the nuclei already formed instead of the formation of new nuclei and therefore led to the formation of larger particles. With the increase of hydrazine concentration, the enhanced reduction rate favored the generation of much more

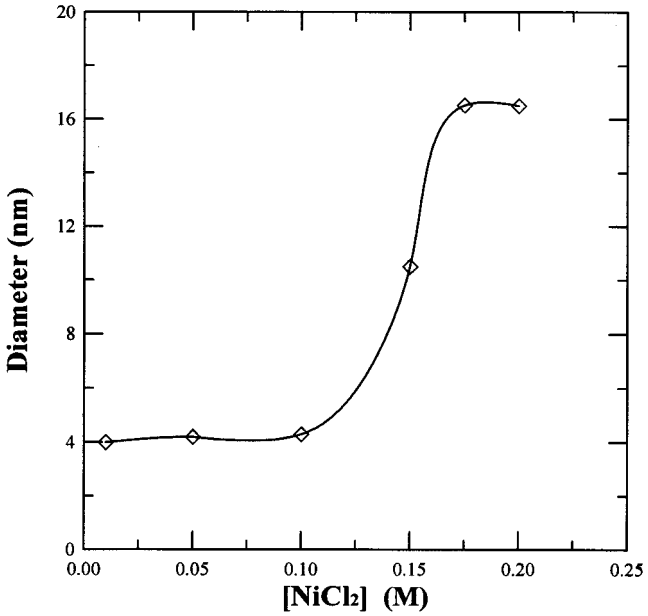

Figure 5. Effect of nickel chloride concentration on the average diameter of nickel nanoparticles. [N_2H_5OH] = 1.0 M; water/CTAB/*n*-hexanol = 22/33/45; 73 °C.

nuclei and the formation of smaller nickel nanoparticles. When the concentration ratio of hydrazine to nickel chloride was large enough (>10), the reduction rate of nickel chloride was much faster than the nucleation rate and almost all nickel ions were reduced to atoms before the formation of nuclei. The nucleation rate was not further raised, and the number of nuclei held constant with the increase of hydrazine concentration. Therefore, the size of the resultant nickel nanoparticles was not further reduced and kept at a constant value.

The effect of nickel chloride concentration on the size of nickel nanoparticles was also investigated in the microemulsion system of water/CTAB/*n*-hexanol = 22/33/45. The concentration of hydrazine in the aqueous phase remained at 1.0 M. As indicated in Figure 5, it was found that the average diameter of nickel nanoparticles was not affected by the increase of nickel chloride concentration when the nickel chloride concentration was below 0.1 M. According to the effect of hydrazine concentration mentioned above, the average diameter of nickel nanoparticles was not affected when the concentration ratio of hydrazine to nickel chloride was above 10. Thus, excluding the effect of hydrazine concentration, the result revealed that the size of nickel nanoparticles was not affected significantly by the nickel chloride concentration when the hydrazine concentration was large enough.

Lufimpadio et al.[31] found that the average diameter of iron boride nanoparticles prepared in the water/CTAB/*n*-hexanol microemulsion system increased with the increase of Fe(III) ion concentration. Nagy[30] reported that the average diameters of both the nickel boride and cobalt boride nanoparticles prepared in the water/CTAB/*n*-hexanol microemulsion system decreased first and then increased with the increase of their corresponding metal salt concentrations. They considered that the formation of the relatively large particles at low ion concentration was due to the fact that only few water pools contained the minimum number of ions required to form a nucleus, and hence only few nuclei were formed at the very beginning of the reduction. When the ion concentration increased, they found that the number of nuclei obtained by reduction increased faster than the total number of ions, and hence the particle size decreased. When more than 80% of the water pools contained two or more ions, they suggested that the size of the resultant particles increased again due to the number of nuclei formed remained quasiconstant with the increase of ion concentration.

The phenomena from the literature above, which is inconsistent with our study, could refer to the difference in the reduction, nucleation, and growth processes. The concentrations of ions and reducing agent affected the reduction rate and the distribution of ions (or atoms) in microemulsions. In addition to the collision energy and the sticking coefficient, the rates of both nucleation and growth were determined mainly by the probabilities of the collisions between several atoms, between one atom and a nucleus, and between two or more nuclei. The former kind of collision related to the nucleation, and the latter two kinds of collision refer to the growth process. As stated above, the probability of the effective collision between one atom and a nucleus was higher than those of the other two collisions since the resultant particles were monodispersed and the size of the resultant particles was determined by the number of the nuclei formed at the very beginning of the reduction. Thus, when the reduction was so large that almost all ions were reduced before the formation of nuclei, the number of nuclei formed was determined by the number of total atoms (or ions), their distribution in microemulsions, and the collision energy and sticking coefficient for nucleation. If the number of nuclei increased faster than that of total ions, smaller particles would be obtained. If the increase of nucleus number was proportional to that of total ion number, the particle size might remain unchanged. When the number of nuclei remained constant or increased slower than that of total ions, the particle size would become larger with the increase of ion concentration. The finding reported by Nagy[30] at low ion concentration might belong to the first condition. The phenomenon observed by Nagy[30] at high concentration and that observed by Lufimpadio et al.[31] could refer to the third condition. For this work, the effect of nickel chloride concentration on the size of nickel nanoparticles at a sufficiently high hydrazine concentration might be described by the second condition.

When the concentration of nickel chloride was above 0.1 M, Figure 5 showed that the average diameters of nickel nanoparticles increased significantly. This phenomenon could be explained by two possible reasons. One was that the hydrazine concentration was relatively lower ([N_2H_5OH]/[$NiCl_2$] < 10) and led to the formation of fewer nuclei at the very beginning of the reduction. The other was that the number of atom formed at the very beginning of the reduction remained constant due to high ion concentration as described in the third condition mentioned above: the atoms formed at the latter period were used for the growth of particles and resulted in the formation of larger particles. No investigation was performed when the concentration of nickel chloride was above 0.12 M because the microemulsion solution became unstable and phase separation occurred.

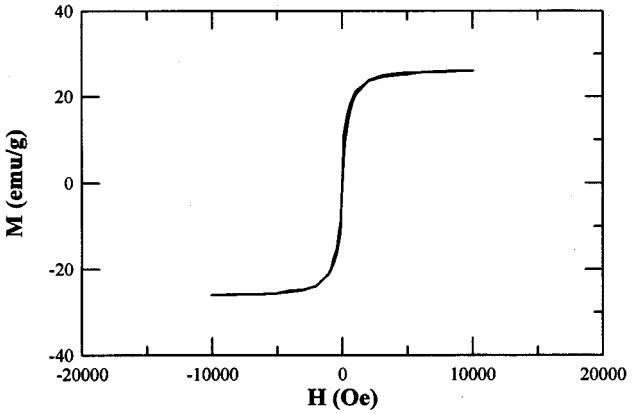

Figure 6. Magnetization versus magnetic field for nickel nanoparticles at 25 °C. Average diameter of nickel nanoparticles was 4.6 nm.

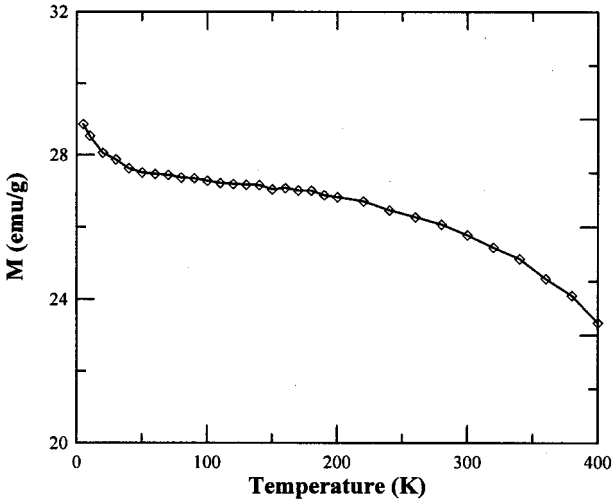

Figure 7. Temperature dependence of the magnetization for nickel nanoparticles at an applied field of 10 kOe. Average diameter of nickel nanoparticles was 4.6 nm.

Magnetic Studies. Nickel has been known to be one of the important magnetic materials. It has been found that the nickel nanoparticles obtained in this work could be precipitated from the suspension by placing a magnet under the beaker. To further investigate the magnetic property of the resultant nickel nanoparticles, a typical sample obtained at a microemulsion system of water/CTAB/*n*-hexanol = 20/30/50 was taken for the magnetic measurement. The magnetization versus magnetic field plots ($M-H$ loops) at 25 °C is shown in Figure 6. The very weak hysteresis revealed the resultant nickel nanoparticles were nearly superparamagnetic. This could be attributed to the fact that the nickel nanoparticles, with an average diameter of 4.6 nm, were so small that they may be considered to have a single magnetic domain. From Figure 6 and its enlargement near the origin, the saturation magnetization (M_s), remanent magnetization (M_r), and coercivity (H_c) could be determined to be 26.2 emu/g, 0.67 emu/g, and 7.5 Oe, respectively.

It is known that the energy of a magnetic particle in an external field is proportional to its size or volume via the number of magnetic molecules in a single magnetic domain. When this energy becomes comparable to thermal energy, thermal fluctuations will significantly reduce the total magnetic moment at a given field.[41] So, the magnetic properties of nanoparticles are usually much smaller than those of the corresponding bulk materials. The M_s, M_r, and H_c values of the bulk nickel at 300 K were about 55 emu/g, 2.7 emu/g, and 100 Oe, respectively.[42] The significant decrease in M_r and H_c of nickel nanoparticles was one of the superparamagnetic characteristics and implied that the thermal energy to demagnetize became dominant over spontaneous magnetization. The saturation magnetization of the nickel nanoparticles was reduced to 48% of the bulk nickel. The disorder structure in amorphous materials and at the interface such as that found at a grain boundary has been shown to cause a decrease in the effective magnetic moment.[42] Therefore, in addition to the thermal fluctuations, the decrease in M_s of nickel nanoparticles also could be attributed to the presence of amorphous structure and the nonmagnetic or weakly magnetic interfaces. Furthermore, the magnetic molecules on the surface lack complete coordination, and the spins are likewise disordered.[41] So, the large surface-to-volume ratio for nanoparticles may be another factor that leads to the decrease in M_s. In addition, the electron exchange between ligand and surface atoms could also quench the magnetic moment.[43] Although the nickel nanoparticles have been washed before the magnetic measurement, the very slight amount of the adsorbed surfactant molecules on the nickel nanoparticles also could cause the decrease in saturation magnetization.

The temperature dependence of the magnetization for the nickel nanoparticles at an applied field of 10 kOe was shown in Figure 7. In the temperature range of 5−400 K, the magnetization increased obviously with the decrease of temperature. This phenomenon could be reasonably considered as a result of the decrease in thermal energy.

Conclusion

The synthesis of nickel nanoparticles in the cationic w/o microemulsion of water/CTAB/*n*-hexanol has been achieved by the reduction of nickel chloride with hydrazine at an elevated temperature, 73 °C. The analyses of electron diffraction pattern and X-ray diffraction showed that the resultant particles were pure nickel crystalline of fcc structure. The effects of microemulsion composition and the concentration of hydrazine and nickel chloride on the particle size have been investigated and discussed in detail. From the study on the effect of microemulsion composition, it was found that the main factor for the preparation of smaller nickel nanoparticles in the water/CTAB/*n*-hexanol system was the higher ratio of CTAB to *n*-hexanol, which could lead to a more rigid interface, instead of the smaller microemulsion droplets. The dependences of particle sizes on the concentrations of hydrazine and nickel chloride

(41) Shafi, K. V. P. M.; Gedanken, A.; Prozorov, R.; Balogh, J. *Chem. Mater.* **1998**, *10*, 3445.
(42) Hwang, J. H.; Dravid, V. P.; Teng, M. H.; Host, J. J.; Elliott, B. R.; Johnson, D. L.; Mason, T. O. *J. Mater. Res.* **1997**, *12*, 1076.
(43) Van Leeuwen, D. A.; Van Ruitenbeek, L. M.; De Jongh, L. J.; Ceriotti; Pacchioni, G.; Häberlen, O. D.; Rösch, N. *Phys. Rev. Lett.* **1994**, *73*, 1432.

could be explained from the reduction, nucleation, and growth processes. It showed that the average diameter of nickel nanoparticles was determined by the number of nuclei formed at the very beginning of reduction. The magnetic measurements indicated that the nickel nanoparticles with an average diameter of 4.6 nm were superparamagnetic. Compared with the bulk nickel, the significant decrease of nickel nanoparticles in the saturation magnetization (26.2 emu/g), remanent magnetization (0.67 emu/g), and the coercivity (7.5 Oe) essentially reflected the nanoparticle nature. Because of the decrease in the thermal energy, the magnetization was observed to increase with the decrease of temperature at 5−400 K.

Acknowledgment. This work was performed under Contract Number NSC 88-2214-E006-017, under the auspices of the National Science Council of the Republic of China, to which the authors wish to express their thanks.

CM991167Y